

## INFRARED ARRAY CAMERA (IRAC) OBSERVATIONS OF PLANETARY NEBULAE

JOSEPH L. HORA,<sup>1</sup> WILLIAM B. LATTER,<sup>2</sup> LORI E. ALLEN,<sup>1</sup> MASSIMO MARENGO,<sup>1</sup> LYNNE K. DEUTSCH,<sup>1,3</sup> AND JUDITH L. PIPHER<sup>4</sup>

Received 2004 March 30; accepted 2004 May 19

### ABSTRACT

We present the initial results from the Infrared Array Camera (IRAC) imaging survey of planetary nebulae (PNs). The IRAC colors of PNs are red, especially in the 8.0  $\mu\text{m}$  band. Emission in this band is likely due to contributions from two strong  $\text{H}_2$  lines and a [Ar III] line in that bandpass. IRAC is sensitive to the emission in the halos as well as in the ionized regions that are optically bright. In NGC 246, we have observed an unexpected ring of emission in the 5.8 and 8.0  $\mu\text{m}$  IRAC bands not seen previously at other wavelengths. In NGC 650 and NGC 3132, the 8.0  $\mu\text{m}$  emission is at larger distances from the central star compared to the optical and other IRAC bands, possibly related to the  $\text{H}_2$  emission in that band and the tendency for the molecular material to exist outside of the ionized zones. In the flocculi of the outer halo of NGC 6543, however, this trend is reversed, with the 8.0  $\mu\text{m}$  emission bright on the inner edges of the structures. This may be related to the emission mechanism, where the  $\text{H}_2$  is possibly excited in shocks in the NGC 6543 halo, whereas  $\text{H}_2$  emission is likely fluorescently excited in the UV fields near the central star.

*Subject headings:* infrared: ISM — planetary nebulae: general — planetary nebulae: individual (Hb 12, NGC 246, NGC 650, NGC 2440, NGC 3132, NGC 6543)

### 1. INTRODUCTION

In recent years the study of stellar ejecta released during final evolutionary stages has provided many new insights into stellar evolution. One reason for these major leaps forward has come from the advancement of near-IR imaging and spectroscopy, as well as space-based platforms (*Hubble Space Telescope* [HST], *Infrared Space Observatory* [ISO]) providing new views of the stellar death process. Mass lost from stars on the asymptotic giant branch (AGB) is observable as the extended envelopes of planetary nebulae (PNs). A significant amount of material released into the ISM by PNs and supernovae is in the form of silicate and carbonaceous dust. Tiny carbon grains, or polycyclic aromatic hydrocarbons (PAHs), have strong emission features throughout much of the near- and mid-IR spectral regions, in addition to numerous atomic and molecular features from ionized and shock heated gas.

Several of the brightest PNs have been imaged in the mid- and near-IR at high spatial resolution from the ground (Hora et al. 1990, 1993; Latter et al. 1995), but the sensitivity of the Infrared Array Camera (IRAC; Fazio et al. 2004) and the other instruments on *Spitzer* (Werner et al. 2004) will allow us to expand our knowledge beyond what was possible on the ground or with previous space missions. *ISO* provided an initial high-sensitivity look at the characteristics of PNs in the mid- and far-IR (Cox et al. 1998; Hora & Deutsch 1999; Fong et al. 2001; Castro-Carrizo et al. 2001). One large nearby PN that was observed by Cox et al. was NGC 7293 (the Helix). The mid-IR emission is dominated by emission from molecular hydrogen in the ground rotational state. The  $\nu = 0-0$   $S(5)$  line

at 6.91  $\mu\text{m}$  (which is the brightest  $\text{H}_2$  line in NGC 7293) and the  $S(4)$  line at 8.02  $\mu\text{m}$  fall within the IRAC 8.0  $\mu\text{m}$  band, so that band is a good tracer of the  $\text{H}_2$  in PN. There will also be  $\text{H}_2$  emission in the other IRAC bands, for example, the  $\nu = 0-0$   $S(7)$  line at 5.51  $\mu\text{m}$  in the 5.8  $\mu\text{m}$  band, the  $S(9)$  line at 4.69  $\mu\text{m}$  in the 4.5  $\mu\text{m}$  band, and a large number of transitions in the 3.6  $\mu\text{m}$  band (Black & van Dishoeck 1987). IRAC also will detect emission from atomic lines present in the bands, e.g. the  $\text{Br}\alpha$  H line at 4.05  $\mu\text{m}$  in the 4.5  $\mu\text{m}$  band, and the 6.98  $\mu\text{m}$  [Ar II] and 8.99  $\mu\text{m}$  [Ar III] line in the IRAC 8.0  $\mu\text{m}$  band. If emission from PAHs at 3.3, 6.2, and 7.7  $\mu\text{m}$  are present, they will contribute to the emission measured in the 3.6, 5.8, and 8.0  $\mu\text{m}$  IRAC bands.

With IRAC, we are conducting a program to observe 35 PNs (Program ID 68). A related project with the Multiband Imaging Photometer for *Spitzer* (MIPS) and Infrared Spectrograph (IRS) instruments led by W. B. Latter (Program ID 77) will obtain 24–160  $\mu\text{m}$  images and 5–40  $\mu\text{m}$  spectra of PNs. In this paper we present images of six of the PNs in the IRAC program, which were the first six objects observed since launch. The PNs are Hubble 12 (Hb 12; *Spitzer* AOR 0004413952), NGC 246 (AOR 0004416256), NGC 650 (AOR 0004421120), NGC 2440 (AOR 0006621440), NGC 3132 (AOR 0004423168), and NGC 6543 (AOR 0004418816).

### 2. OBSERVATIONS AND DATA REDUCTION

The IRAC observations were obtained using the 30 s High Dynamic Range (HDR) mode. This mode takes pairs of images with 1.2 and 30 s frame times at each position in all four channels (3.6, 4.5, 5.8, and 8.0  $\mu\text{m}$ ; see Fazio et al. 2004, for definitions of the bands). Between 5 and 18 dither positions were obtained on each source. For objects that did not approach saturation, the 30 s frame time data were used. For the objects that were close to or above saturation in 30 s, the 1.2 s frames were mosaicked and used to fill in the brightest regions of the images.

The Basic Calibrated Data (BCD) products from the *Spitzer* Science Center (SSC) pipeline were used to construct the

<sup>1</sup> Harvard-Smithsonian Center for Astrophysics, 60 Garden Street, MS 65, Cambridge, MA 02138-1516; jhora@cfa.harvard.edu.

<sup>2</sup> *Spitzer* Science Center, MC 220-6, California Institute of Technology, Pasadena, CA 91125.

<sup>3</sup> Deceased (2004 April 2). Lynne will be deeply missed by her friends and colleagues on the IRAC team.

<sup>4</sup> Department of Physics and Astronomy, University of Rochester, Rochester, NY 14627-0171.

TABLE 1  
PLANETARY NEBULAE MAGNITUDES

Source (1)	Aperture (arcsec) (2)	[3.6] (3)	[4.5] (4)	[5.8] (5)	[8.0] (6)
Hb 12 .....	24.4 <sup>a</sup>	6.94	5.98	5.10	2.61
NGC 246.....	305 <sup>b</sup>	8.91	7.80	7.59	5.77
NGC 650.....	91.5 <sup>b</sup>	9.72	8.51	8.78	6.93
NGC 2440.....	81 <sup>b</sup>	7.83	7.02	6.05	4.19
NGC 3132.....	130 <sup>b</sup>	7.79	7.13	6.65	5.25
NGC 6543.....	48.8 <sup>a</sup>	7.56	6.59	6.87	4.32
NGC 246neb.....	305 <sup>b</sup>	8.97	7.82	7.60	5.77
NGC 3132neb.....	130 <sup>b</sup>	7.92	7.21	6.69	5.26
NGC 6543knot.....	92 × 52 <sup>c</sup>	11.11	10.09	9.33	7.75
NGC 246-cstar.....	3 <sup>a</sup>	12.02	12.10	12.01	11.86
NGC 650-cstar.....	3 <sup>a</sup>	16.06	15.70	16.42	16.54
NGC 3132-cstar.....	3 <sup>a</sup>	10.09	9.98	10.00	10.32

<sup>a</sup> Circular aperture diameter.

<sup>b</sup> Square aperture width.

<sup>c</sup> Long dimension is horizontal direction in orientation shown in Fig. 1.

mosaic images for all objects. The BCD products have the instrumental signatures removed from the data and are calibrated in units of MJy sr<sup>-1</sup>, based on the calibration derived during the first few months of the mission from measurements of standard stars (Fazio et al. 2004; Hora et al. 2004). Two further reduction steps were performed on the BCD. First, a sky background frame was constructed from the median of the off-source images and subtracted from the BCD frames. Next, some artifacts in the pipeline images caused by bright stars were removed by forcing the column or row median in regions with no sources to be equal to that of adjacent columns or rows. The individual BCD images were combined into a single image for each channel and frame time using the SSC mosaicker. The final images have a linear pixel size 1/4 that of the input pixels (1/16 of the area). For flux calibration, the zero-magnitude fluxes in the IRAC bands were taken to be 277.5, 179.5, 116.6, and 63.1 Jy for channels 1–4, respectively. A correction for the extended emission was applied to the fluxes as described in the *Spitzer* Observer’s Manual.<sup>5</sup>

### 3. RESULTS AND DISCUSSION

The IRAC images of the nebulae are presented in Figures 1 and 2 (Plates 1 and 2). Color images of five of the PNs are shown in Figure 1. The color images are composites of all four IRAC bands, as described in the figure caption. Images of the individual bands are shown in Figure 2.

#### 3.1. IRAC Colors of PN

The Vega-relative magnitudes and colors of the PNs presented in this paper are shown in Table 1. The magnitude for each nebula was estimated by summing all of the detectable emission from the nebula or the particular component and subtracting the emission from the field stars in that part of the image. Column (2) indicates the size and shape of the area summed, centered on the central star of the PN. In general, the total field star flux was small compared to the nebular flux, ranging from ~1.5% in the 3.6 μm band for a couple of the PNs to less than 3% in the 8.0 μm band. Where it was possible to

extract the central star separately from the PN, those magnitudes and colors are also presented, as well as the nebula without the central star. Since the nebulae dominate the flux from the object, the nebula-alone colors are almost the same as the total object colors.

The IRAC color data are plotted in Figure 3. The [3.6] – [4.5] color is in the ~0.6–1.2 range for the sample, and the [5.8] – [8.0] color is in the ~1.4–2.5 range. A typical error bar for the nebula is shown for one of the points; calibration uncertainties at this time early in the mission are thought to be 0.1 mag or less in all channels. Some of the [5.8] – [8.0] colors are redder than expected; for example, Whitney et al. (2003) predicted [5.8] – [8.0] PN colors of less than 2. The red [5.8] – [8.0] color is possibly due to several factors, including continuum emission from warm dust (e.g., Hb 12), or line emission from forbidden atomic lines or H<sub>2</sub> lines in the broad 8 μm band (e.g., NGC 6543; see discussion below).

The *ISO* SWS (Kessler et al. 1996; de Graauw et al. 1996) spectra of three of the PNs are shown in Figure 4. The full spectrum of NGC 2440 was presented by Bernard-Salas et al. (2002). We show these spectra as representative spectra from some of the PNs in the mid-IR. Several atomic and H<sub>2</sub> line positions are shown, not necessarily identifying them in the spectrum, but to indicate their position relative to the IRAC bands. No PAH emission is seen in the PN spectra shown in Figure 4. In addition, the colors of the PNs presented here are much redder than expected if the emission was caused by only PAH lines (Li & Draine 2001).

#### 3.2. Individual Nebulae

##### 3.2.1. Hb 12

Hb 12 is a young bipolar PN with a complex inner structure inside the bipolar lobes, all of which is seen in fluorescently excited H<sub>2</sub> emission in the near-IR (Hora & Latter 1996). The IRAC image shows very little extended emission near the core, so the images are not presented here. The *ISO* spectrum in Figure 4 shows a rising continuum toward longer wavelengths, which is consistent with the observed IRAC colors. H<sub>2</sub> lines are also present—for example, the 0–0 S(5) line at 6.91 μm and forbidden lines such as [Ar III] at 8.99 μm.

<sup>5</sup> See <http://ssc.spitzer.caltech.edu/documents/som>.

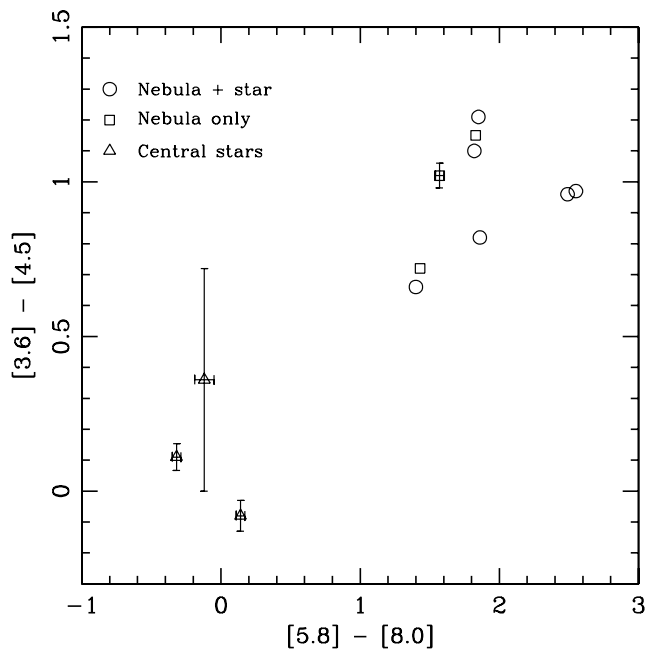


FIG. 3.—Planetary nebulae colors from the IRAC data in Table 1. The total nebula plus central star, nebula-alone, and central star-alone colors are plotted, for those nebulae for which it was possible to separate them out. For NGC 6543, the color of the brightest knot in the extended halo is shown. The error bars for the central stars are shown for each point, and a representative error bar for the nebulae are shown for one point for clarity.

### 3.2.2. NGC 246

NGC 246 is an oval-shaped, high-excitation PN approximately  $4.5''$  in diameter. Recently, Szentgyorgyi et al. (2003) imaged NGC 246 in several near-UV lines and detected structure in the inner parts of the nebula. In particular, the image in the  $[\text{Ne v}]$  line at  $342.9 \text{ nm}$  shows bright arcs near the central star in an “hourglass” or bipolar structure near, but not centered on, the central star. The remarkable feature in the IRAC images is the oval structure that appears brightest in the  $5.8$  and  $8.0 \mu\text{m}$  bands. This is possibly an inclined ring and is not centered on the central star or the outer shell of the nebula. The brightest part of the PN is the C-shaped feature to the southeast of the central star, which is also brightest in the  $[\text{Ne v}]$  image. The cavity that forms the northern part of the hourglass is evident in the IRAC images, particularly the  $4.5 \mu\text{m}$  band, but is not as distinct as in the UV image.

### 3.2.3. NGC 650

NGC 650 is a large, high-excitation PN with bipolar structure. The kinematic study of Bryce et al. (1996) showed that there are several components, including a central ring with two attached inner lobes, and outer lobes with much lower expansion velocities, and a higher velocity polar cap on the southeast side. In the near-IR, the emission is dominated by  $\text{H}_2$  that is brightest in the central  $2''$  region (Kastner et al. 1996).

All of the major components are seen in at least one of the IRAC bands. The IRAC bands likely contain emission from  $\text{H}_2$  as well as atomic lines. The emission seen in the  $8.0 \mu\text{m}$  band is more extended in the central ring and the lobes than the shorter bands, as evidenced by the reddish color on the outer edges seen in Figure 1. The  $8.0 \mu\text{m}$  emission in the southwest extends toward the wall of one of the lobes, giving it the appearance of a red arrow pointing to the southwest. The

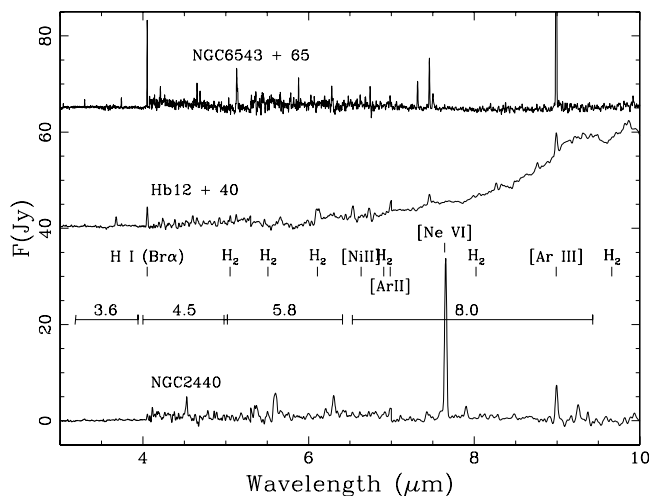


FIG. 4.—Spectra of Hb 12, NGC 2440, and NGC 6543, from *ISO* observations 43700330, 72501762, and 02400714, respectively. These are based on the online pipeline products downloaded from the *ISO* database. The spectra of NGC 6543 and Hb 12 have been offset vertically by the indicated amounts. Some of the atomic and  $\text{H}_2$  lines have been indicated. Also shown are the wavelength ranges between the half-power points of the IRAC bands. See Fazio et al. (2004) for details on the IRAC spectral response function.

$\text{H}_2$  emission in other PNs, for example, M2–9 (Hora & Latter 1994) or NGC 7027 (Latter et al. 1995), is predominantly on the outer edges of the nebula, delineating the ionization front. Bryce et al. (1996) detected a polar cap in the southeast part of the nebula with a higher velocity than the surrounding shell. The cap is faintly visible in the IRAC bands, clearest in the  $8.0 \mu\text{m}$  image. We see a faint extended structure on the northwest side that could be the opposing cap. In addition,  $\sim 50''$  to the southeast of the central star there are three small emission features about  $5''$  long, oriented radially from the central star. They are bluer than the other features and could be material ejected along the poles of the PN.

### 3.2.4. NGC 2440

The PN NGC 2440 is a high-excitation, point-symmetric nebula with at least three sets of opposing knots of emission. Around the inner parts of the nebula is a circular shell of emission, not centered on the symmetric inner structure. There are radial “spokes” of emission extending from the central knots to the outer circular ring at several locations. These structures are all seen in  $\text{H}_2$  emission in the near-IR (Latter et al. 1995; Latter & Hora 1997). The appearance in the IRAC bands is similar, with all the major features apparent. The relative brightness of the features varies in the bands, with the outer shell much fainter at the longer wavelengths. The *ISO* spectrum does not show any bright emission lines, except possibly the  $7.64 \mu\text{m}$  line of  $\text{Ne v}$ , which would be detected in the  $8.0 \mu\text{m}$  band.

### 3.2.5. NGC 3132

NGC 3132 appears ellipsoidal in low-resolution images; however, a simple shell model does not explain all of the observed characteristics. Monteiro et al. (2000) propose a model in which the nebula has an hourglass structure that is being viewed at  $40^\circ$  relative to the light of sight. This structure explains the details of the morphology and the low central density observed in the optical images.

The IRAC images are similar to the optical and near-IR in the central regions, with the  $8.0 \mu\text{m}$  emission relatively

brighter in the outer regions. One interesting feature in the IRAC images is the faint extended emission approximately north-south along the major axis of the bright shell. There are what appear to be partial rings, and filaments connecting the rings radially with respect to the central star, and many knots and loops of emission that extend up to approximately 3 times the size of the bright optical nebula. It is surprising, given the proposed model, that this extended emission would appear along this axis, rather than the perpendicular axis where the major axis of the lobes are proposed to exist. In fact, the nebula does not appear to extend very much at all in the east-west direction beyond the bright optical nebula.

### 3.2.6. NGC 6543

NGC 6543 (the Cat's Eye) is another point-symmetric nebula with a complex set of bubbles, rings, shock fronts, jets, and fast, low-ionization emission-line regions (FLIERs; see Balick et al. 1993, 1994). These are most clearly visible in the *HST* images of this PN, e.g., in lines of [N II] and [O III] (Reed et al. 1999). The near-IR appearance is similar to the optical (Latter et al. 1995), with the prominent features being the oval-shaped rings at right angles to each other. The IRAC images are similar to the near-IR and optical broadband images, also showing the oval rings as the main features. The FLIERs are more prominent at these wavelengths, especially in the 5.8 and 8.0  $\mu\text{m}$  bands. The *ISO* spectrum of NGC 6543 shows bright lines of H (Br $\alpha$  at 4.05  $\mu\text{m}$ ) and [Ar III] at 8.99  $\mu\text{m}$ , which might affect the flux in the 4.5 and 8.0  $\mu\text{m}$  bands, but otherwise the emission is not detected in the 3–10  $\mu\text{m}$  range of the *ISO* spectrum in Figure 4.

In addition to the bright inner region, there is a faint roughly circular halo extending to a radius of approximately 170'' (Balick et al. 1992, 2001). The halo has a faint smooth component, but near the nebula exhibits concentric rings in [O III], and the outer rim is dominated by cometary-shaped “floculi,” the brightest being directly west of center. The appearance of the core and outer halo is similar in the IRAC bands (the concentric rings are not observable at IRAC's angular resolution). There are some differences between the optical and

IRAC images in the structure of the largest knot. The knot is relatively brighter at longer wavelengths, and the peak moves farther away from the center as one moves longer in wavelength. In the 8.0  $\mu\text{m}$  image, the brightest spot appears behind the front of the cometary front, and there is much more structure south of the knot. Recent ground-based images (J. L. Hora 2004, in preparation) show that the knot has significant H<sub>2</sub> emission at 2.12  $\mu\text{m}$ , so there is likely some emission from the 0–0 *S*(7) line in the 5.8  $\mu\text{m}$  band and the *S*(4) and *S*(5) lines in the 8.0  $\mu\text{m}$  band.

## 4. CONCLUSIONS

The IRAC colors of PNs are red, especially in the 8.0  $\mu\text{m}$  band, which is likely due to contributions from two strong H<sub>2</sub> lines and a [Ar III] line in that bandpass, in addition to thermal continuum emission from dust. PAH emission is not detected in the objects presented here but is expected to be present in other PNs. In NGC 246, we have observed an unexpected ring of emission in the 5.8 and 8.0  $\mu\text{m}$  IRAC bands not seen previously at other wavelengths. In NGC 650 and NGC 3132, the 8.0  $\mu\text{m}$  emission is at larger distances from the central star compared to the optical and other IRAC bands, possibly related to the H<sub>2</sub> emission in that band and the tendency for the molecular material to exist outside of the ionized zones. In the flocculi of the outer halo of NGC 6543, however, the 8.0  $\mu\text{m}$  emission is brightest on the inner edges of the structures. This may be related to the emission mechanism, where the H<sub>2</sub> is possibly excited in shocks in the NGC 6543 halo, whereas the emission is likely fluorescently excited in the UV fields near the central star.

This work is based on observations made with the *Spitzer Space Telescope*, which is operated by JPL, Caltech, under NASA contract 1407. Support for this work was provided by NASA through Contract 1256790 issued by JPL/Caltech. Support for the IRAC instrument was provided by NASA through Contract 960541 issued by JPL.

## REFERENCES

- Cox, P., et al. 1998, *ApJ*, 495, L23  
 Balick, B., Gonzalez, G., Frank, A., & Jacoby G. 1992, *ApJ*, 392, 582  
 Balick, B., Perinotto, M., Maccioni, A., Terzian, Y., & Hajian, A. 1994, *ApJ*, 424, 800  
 Balick, B., Rugers, M., Terzian, Y., & Chengalur, J. N. 1993, *ApJ*, 411, 778  
 Balick, B., Wilson, J., Hajian, A. R. 2001, *AJ*, 121, 354  
 Bernard-Salas, J., Pottasch, S. R., Feibelman, W. A., & Wesselius, P. R. 2002, *A&A*, 387, 301  
 Black, J. H., & van Dishoeck, E. F. 1987, *ApJ*, 322, 412  
 Bryce, M., Mellema, G., Clayton, C. A., Meaburn, J., Balick, B., & Lopez, J. A. 1996, *A&A*, 307, 253  
 Castro-Carrizo, A., Bujarrabal, V., Fong, D., Meixner, M., Tielens, A. G. G. M., Latter, W. B., & Barlow, M. J. 2001, *A&A*, 367, 674  
 de Graauw, T. et al 1996, *A&A*, 315, L49  
 Fazio, G. G., et al. 2004, *ApJS*, 154, 10  
 Fong, D., et al. 2001, *A&A*, 367, 652  
 Hora, J. L., & Deutsch, L. K. 1999, in *The Universe as seen by ISO*, ed. P. Cox, V. Demuyt, & M. Kessler (ESA Pub. Div.; Noordwijk: ESTEC), 337  
 Hora, J. L., Deutsch, L. K., Hoffmann, W. F., & Fazio, G. G. 1990, *ApJ*, 353, 549  
 Hora, J. L., Deutsch, L. K., Hoffmann, W. F., & Fazio, G. G. 1993, *ApJ*, 413, 304  
 Hora, J. L., & Latter, W. B. 1994, *ApJ*, 437, 281  
 ———. 1996, *ApJ*, 461, 288  
 Hora, J. L., et al. 2004, *Proc. SPIE*, 5487, in press  
 Kastner, J. H., Weintraub, D. A., Gatley, I., Merrill, K. M., & Probst, R. G. 1996, *ApJ*, 462, 777  
 Kessler, M. F., et al. 1996, *A&A*, 315, L27  
 Latter, W. B., & Hora, J. L. 1997, in *I.A.U. Symposium 180, Planetary Nebulae*, ed. H. J. Habing & H. J. G. L. M. Lamers (Dordrecht: Kluwer), 254  
 Latter, W. B., Kelly, D. M., Hora, J. L., & Deutsch, L. K. 1995, *ApJS*, 100, 159  
 Li, A., & Draine, B. T. 2001, *ApJ*, 554, 778  
 Monteiro, H., Morisset, C., Gruenwald, R., & Viegas, S. M. 2000, *ApJ*, 537, 853  
 Reed, D. S., et al. 1999, *AJ*, 118, 2430  
 Szentgyorgyi, A., Raymond, J., Franco, J., Villaver, E., & Lopez-Martin, L. 2003, *ApJ*, 594, 874  
 Werner, M., et al. 2004, *ApJS*, 154, 1  
 Whitney, B. A., Wood, K., Bjorkman, J. E., & Cohen, M. 2003, *ApJ*, 598, 1079

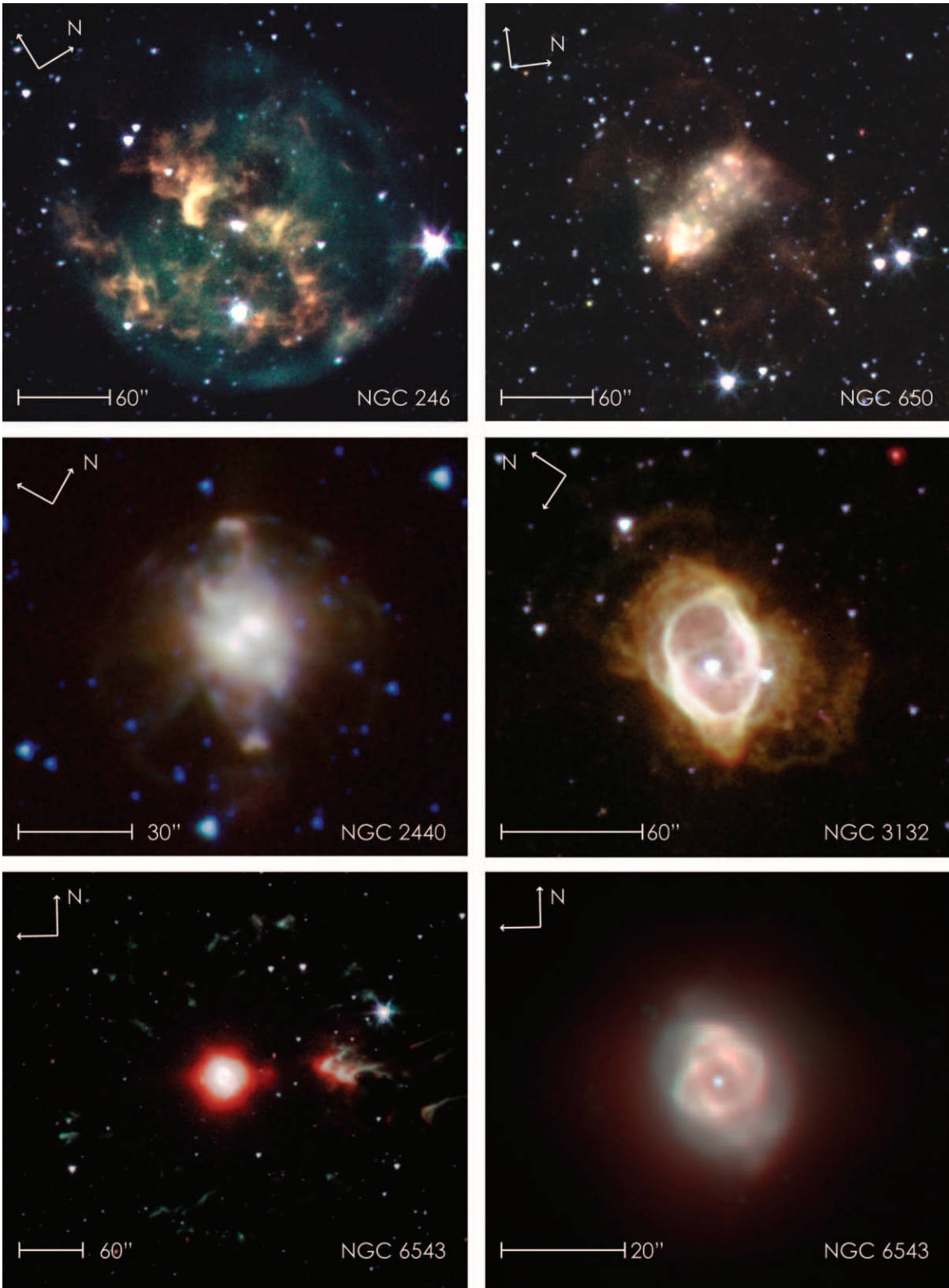


FIG. 1.—Planetary nebulae color images. The image orientations and scales are shown on each image. The images are displayed in a histogram-equalized color scale (with the exception of the close-up of NGC 6543, which uses a square-root color scale). The four IRAC bands have been reduced into the RGB color space using the following scheme: IRAC 8.0  $\mu\text{m}$  = “red,” IRAC 5.8  $\mu\text{m}$  = “cyan,” IRAC 4.5  $\mu\text{m}$  = “yellow-green,” IRAC 3.6  $\mu\text{m}$  = “purple.”

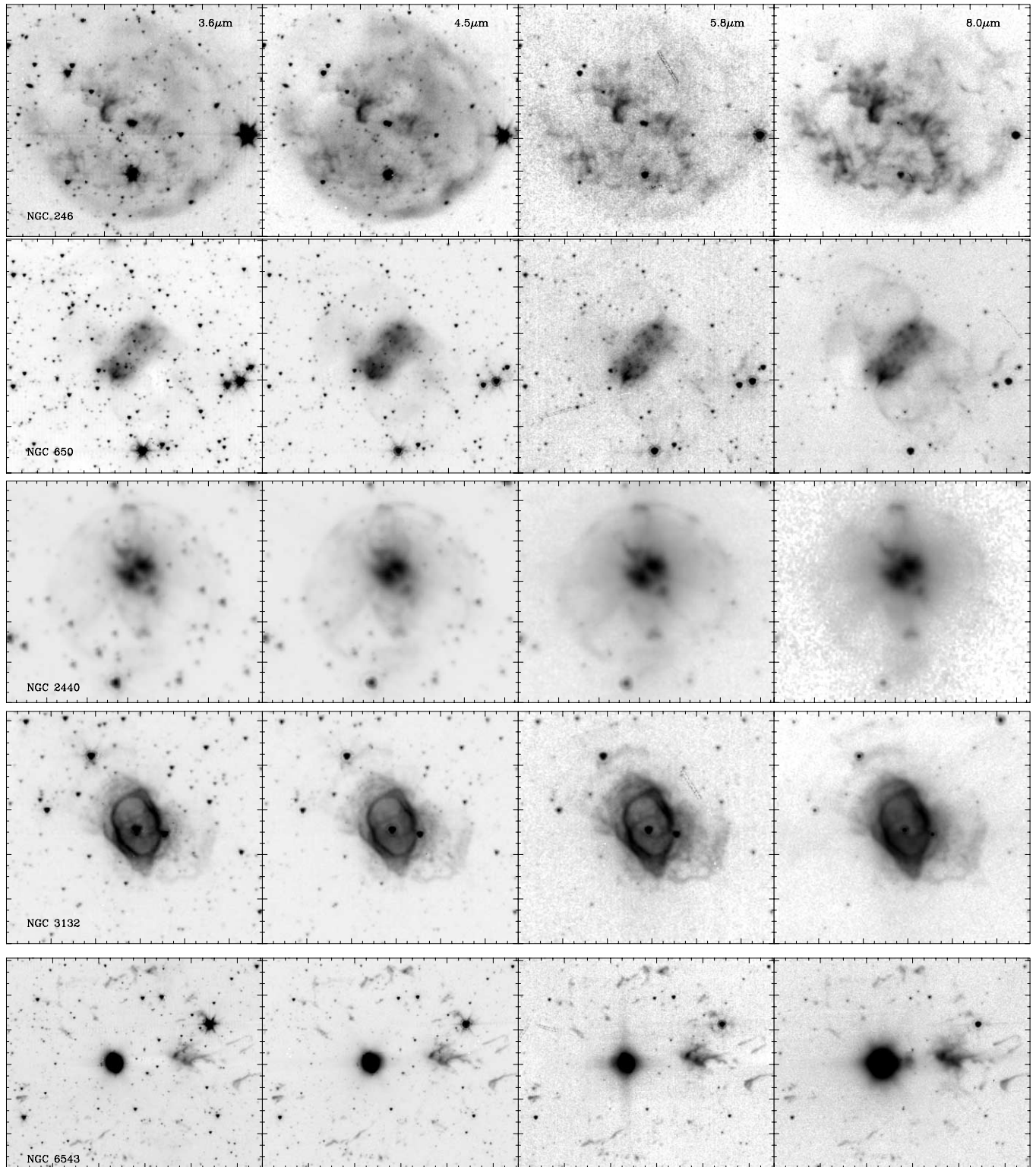


FIG. 2.—Planetary nebulae images, single IRAC bands. The images are arranged with each object in one row, with the four columns being the IRAC 3.6, 4.5, 5.8, and 8.0  $\mu\text{m}$  bands. The orientations are the same as in Fig. 1. The images are scaled logarithmically, with the peak level set to the brightest part of the extended emission in the image. The image width for each PN is as follows: NGC 246, 287"; NGC 650, 302"; NGC 2440, 116"; NGC 3132, 210"; and NGC 6543, 406".